

# Sachs-Wolfe effect in some anisotropic models

Paulo Aguiar <sup>\*</sup> and Paulo Crawford <sup>†</sup>

Centro de Astronomia e Astrofísica da Universidade de Lisboa  
Campo Grande, Ed. C8; 1749-016 Lisboa, Portugal

## Abstract

In this work it is shown for some spatially homogeneous but anisotropic models how the inhomogeneities in the distribution of matter on the surface of the last scattering produce anisotropies in large angular scales (larger than  $\vartheta \gtrsim 2^\circ$ ) which do not differ from the ones produced in Friedmann-Lemaître-Robertson-Walker (FLRW) geometries. That is, for these anisotropic models, the imprint left on the cosmic microwave background radiation (CMBR) by the primordial density fluctuations, in the form of a fractional variation of the temperature of this radiation, is governed by the same expression as the one given for FLRW models. More precisely, under adiabatic initial conditions, the classical Sachs-Wolfe effect is recovered, provided the anisotropy of the overall expansion is small. This conclusion is in agreement with previous work on the same anisotropic models where we found that they may go through an ‘isotropization’ process up to the point that the observations are unable to distinguish them from the standard FLRW model, if the Hubble parameters along the orthogonal directions are assumed to be approximately equal at the present epoch. Here we assumed upper bounds on the present values of anisotropic parameters imposed by COBE observations.

## 1 Introduction

The task of proving the homogeneity and isotropy of the Universe at large scales is not a simple one. It is generally accepted that the Universe is spatially homogeneous as a result of the so called Copernican principle, that is, the assumption that we live in a typical place. Then, a fundamental result follows from this principle that if the CMBR temperature were exactly isotropic about our position, it should be exactly isotropic about every point in spacetime, and the universe would have to be exactly an FLRW model. This was proved by Ehlers, Geren and Sachs [1], and known as the EGS theorem.

As a matter of fact, observations indicate that the temperature of the CMBR is isotropic to a remarkable degree. This observation, put together

---

<sup>\*</sup>paguiar@cosmo.fis.fc.ul.pt

<sup>†</sup>crawford@cosmo.fis.fc.ul.pt

with the Copernican principle, leads to the widespread belief that the Universe can be accurately described by a spatially homogeneous and isotropic model on sufficiently large scales, drastically reducing the space of solutions of Einstein equations, and the number of possible cosmological models.

However, the EGS theorem is not directly applicable to the real Universe since the CMBR temperature is not exactly isotropic. This fact might explain why, despite the high level of isotropy of CMBR temperature, some authors have worked on spatially homogeneous but anisotropic models to analyze whether they might agree with present observations, in particular with those models which could be considered to be close to FLRW. Recall that one defines to be ‘close’ to a FLRW model when both parameters

$$\mathcal{W}^2 = \frac{E_{ab}E^{ab} + H_{ab}H^{ab}}{6H^4}, \quad (1)$$

$$\Sigma^2 = \frac{\sigma_{ab}\sigma^{ab}}{6H^2} \quad (2)$$

are almost zero, although the former usually receives more attention than the latter in the astrophysical literature, as was stressed in [2]. Here,  $\sigma_{ab}$  is the shear tensor,  $H$  is the mean Hubble parameter,  $E_{ab}$  and  $H_{ab}$  are the electric and magnetic part of the Weyl tensor, respectively, and we refer to  $\Sigma$  as the shear parameter and to  $\mathcal{W}$  as the Weyl parameter. Note that for non-tilted spatially homogeneous perfect fluid models, a zero shear tensor implies that the Weyl curvature tensor is zero, and thus characterizes the FLRW models, that is,  $\Sigma = 0 \Rightarrow \mathcal{W} = 0$ . However, restricting  $\Sigma$  to be small does not guarantee that  $\mathcal{W}$  is small since the Weyl curvature tensor is related to time derivatives of the shear tensor and these need not be small compared to  $H^2$ . It is thus of considerable interest to note that the EGS theorem might be extended as was done in [3], given some reasonable assumptions, by replacing the word “exactly” by “almost”, thus obtaining an “almost” EGS theorem. In other words, they showed, given certain assumptions, that if the CMBR temperature is measured to be almost isotropic in a spacetime region of an expanding universe, then the universe is close to an FLRW model in that region. In terms of the previously introduced anisotropy parameters, the condition for the universe to be close to an FLRW model becomes

$$\Sigma \ll 1, \quad \mathcal{W} \ll 1. \quad (3)$$

It should be stressed, however, that in [4] it is shown that there are spatially homogeneous cosmological models such that the CMBR temperature is measured to be isotropic at a given time  $t_0$  by all fundamental observers, even though the overall expansion of the universe is highly anisotropic at  $t_0$ , here assumed to be present time.

On the other hand, if the classical tests of cosmology are applied to a simple Kantowski-Sachs metric and the results compared with those obtained for the standard model, the observations will not be able to distinguish between these models if the Hubble parameters along the orthogonal directions

are assumed to be approximately equal [5] at  $t_0$ , that is, if  $\Sigma \approx 0$ . Following along the same lines, we made a qualitative study [6] of three axially symmetric metrics (Kantowski-Sachs, Bianchi type-I and Bianchi type-III), with a cosmological constant and dust, to analyze which were physically permitted, when we assume them to be bound by a high degree of isotropy, from the point of view of overall expansion. More specifically, although our geometries described anisotropic cosmological fields they could be considered to be almost FLRW as far as its overall expansion, since the shear tensor was close to zero, at least since the time of last scattering. We found that these models undergo ‘isotropization’ up to the point that the observations will not be able to distinguish between them and the standard model, except for the Kantowski-Sachs model ( $\Omega_{k_0} < 0$ ) and for the Bianchi type-III model ( $\Omega_{k_0} > 0$ ) with  $\Omega_{\Lambda_0}$  smaller than some critical value  $\Omega_{\Lambda_M}$  [6] (see the definitions of  $\Omega_{k_0}, \Omega_{\Lambda_0}, \Omega_{M_0}$  in [7]). From this analysis we concluded that these models are good candidates for the description of the observed Universe, provided that the Hubble parameters are approximately equal at the last scattering (see computations below). In other words, the low values of the first parameter,  $\Sigma$ , is sufficient to assure a FLRW-like behavior, and the statement that the expansion is highly isotropic means that  $\Sigma \ll 1$ .

Historically, the detection of the CMBR has led to constraints in theoretical models in the field of Cosmology, and favored the Big Bang solutions. Indeed, it was the observed level of isotropy of the CMBR temperature, first detected by Penzias & Wilson [8], which has been considered to provide the best evidence for the large-scale isotropy of the Universe, and still is the strongest argument in favor of an isotropically expanding Universe. Later, more precise experiments proved that this radiation has temperature fluctuations, or anisotropies. These small anisotropies are thought to give rise to the observed galaxies, and large-scale structures in the Universe.

In 1992, the COBE (COsmic Background Explorer) satellite [9, 10] observed the CMBR with unprecedented precision and revealed for the first time that the level of the CMBR temperature fluctuations on large scales is as small as  $\frac{\Delta T}{T} \simeq 10^{-5}$  [11, 12]. After COBE many other ground and balloon born experiments [13], with higher angular resolution, confirmed this result and allowed us to probe the level of the anisotropies on a large range of scales.

On large angular scales, the CMBR anisotropies ( $\frac{\Delta T}{T}$ ), are dominated by the Sachs-Wolfe effect. This phenomenon, already deduced theoretically by Sachs & Wolfe [14], was used to compute the first-order perturbations in a FLRW universe with a flat 3-space filled either with dust or radiation. This is just one of the various possible sources of anisotropy, which occurs when there are inhomogeneities in the distribution of matter on the surface of the last scattering, that may produce anisotropies by the redshift or blueshift of photons. In this paper we compute the Sachs-Wolfe effect [14] for some anisotropic but homogeneous models (Kantowski-Sachs and Bianchi type-III model which is also locally rotationally symmetric (LRS)) and find that under the assumption  $H_{a_0} \simeq H_{b_0}$  (we considered a small anisotropy imposed

by COBE observations: see [7] for details) these models allow us to recover the classic Sachs-Wolfe effect obtained for FLRW universes. This is an interesting result which tells us that CMBR observations on large angular scales will not be able to distinguish these anisotropic models from FLRW ones.

## 2 The method

As Collins and Hawking [15] pointed out, the number of cosmological solutions which demonstrate exact isotropy well after the Big Bang origin of the Universe is a small fraction of the set of allowable solutions to the Einstein equations. It is therefore prudent to take seriously the possibility that the Universe is expanding anisotropically and to investigate what effect anisotropic expansion will have on the angular distribution of background radiation [13]. In this work we show that, for large angular scales ( $\vartheta \gtrsim 2^\circ$ ), there exist homogeneous but anisotropic models, where the photons travelling to an observer from the last scattering surface encounter metric perturbations which cause them to change frequency, just like in the case of FLRW models.

The metrics we consider are Kantowski-Sachs and LRS Bianchi type-III model, given by

$$d\tilde{s}^2 = -dt^2 + a^2(t)dr^2 + b^2(t)(d\theta^2 + f^2(\theta)d\phi^2), \quad (4)$$

where

$$f(\theta) = \begin{cases} \sin \theta & \text{for Kantowski-Sachs} \\ \sinh \theta & \text{for Bianchi type-III} \end{cases}$$

We evaluate the Sachs-Wolfe effect [14, 16], assuming small perturbations in the previous metrics, and then integrating the geodesic equations for the CMBR photons along their paths, from the Last Scattering Surface (LSS) to the observer. In this work we account for the “kinematics effects” undergone by the free propagating radiation from the last scattering, in a perturbed universe, and for the “intrinsic effects” originated by the set of physical and microphysical processes related to the density perturbations in the LSS. For simplicity, it is common to perform a conformal transformation <sup>1</sup> of the previous metrics, and to work with the following metric forms

$$d\bar{s}^2 = -d\eta^2 + dr^2 + \frac{b^2(\eta)}{a^2(\eta)}(d\theta^2 + f^2(\theta)d\phi^2) \quad (5)$$

such that  $d\bar{s}^2$ :  $d\tilde{s}^2 = a^2(\eta)d\bar{s}^2$ , since the null geodesics are preserved by this transformation. Afterwards, the results are transported to  $d\tilde{s}^2$  metric. The

---

<sup>1</sup>Owing to this transformation,  $\eta$  is usually called the conformal time, and it is related to cosmological proper time by  $dt^2 = d\eta^2 a^2(\eta)$ .

metric  $d\bar{s}^2$  is perturbed in the following way

$$\begin{aligned}
d\bar{s}^2 = & -(1+h_{00})d\eta^2 + (1+h_{11})dr^2 + \frac{b^2(\eta)}{a^2(\eta)} \left[ (1+h_{22})d\theta^2 \right. \\
& + (1+h_{33})f^2(\theta)d\phi^2 \left. \right] - (h_{01}+h_{10})d\eta dr - \frac{b(\eta)}{a(\eta)}(h_{02}+h_{20})d\eta d\theta \\
& - \frac{b(\eta)}{a(\eta)}f(\theta)(h_{03}+h_{30})d\eta d\phi + \frac{b(\eta)}{a(\eta)}(h_{12}+h_{21})dr d\theta \\
& + \frac{b(\eta)}{a(\eta)}f(\theta)(h_{13}+h_{31})dr d\phi + \frac{b^2(\eta)}{a^2(\eta)}f(\theta)(h_{23}+h_{32})d\theta d\phi, \quad (6)
\end{aligned}$$

where  $h_{ab}$  are functions of time and position and such that  $h_{ab} \ll 1$ .

Considering the geodesics equation for the photons

$$\frac{d\bar{U}_a}{dw} = \frac{1}{2}\bar{g}_{bc,a}\bar{U}^b\bar{U}^c, \quad (7)$$

where  $\bar{U}^a$  represents the photon 4-vector velocity components and  $w$  the affine parameter associated to its trajectory, we may calculate this 4-velocity integrating the previous equation

$$\bar{U}_a = \frac{1}{2} \int \bar{g}_{bc,a} \bar{U}^b \bar{U}^c dw + {}_{(0)}\bar{U}_a. \quad (8)$$

The term  ${}_{(0)}\bar{U}_a$  represents the non perturbed photon 4-velocity components in the covariant form.

A material observer, moving with some 3-velocity  $\vec{V}$ , in a perturbed universe (metric  $\bar{g}_{ab}$ ), has a 4-velocity given by

$$\bar{V}^a \simeq \left( 1 - \frac{1}{2}h_{00}, \bar{V}^1, \bar{V}^2, \bar{V}^3 \right). \quad (9)$$

This observer measures a photon energy  $\bar{E}_\gamma$  proportional to  $\bar{U}_a \bar{V}^a$ ,

$$\bar{E}_\gamma \propto \left( \frac{1}{2} \int \bar{g}_{bc,a} \bar{U}^b \bar{U}^c dw + {}_{(0)}\bar{U}_a \right) \left( 1 - \frac{1}{2}h_{00}, \bar{V}^i \right). \quad (10)$$

Decomposing the 4-velocity in a Taylor expansion and conserving only the first order term  $\bar{U}^a \simeq {}_{(0)}\bar{U}^a + {}_{(1)}\bar{U}^a$  (it can be shown that the 4-velocity, in covariant and contravariant components, is given by  ${}_{(0)}\bar{U}^a = (1, \sqrt{\alpha}, a^2/b^2 \sqrt{\beta}, 0)$  and  ${}_{(0)}\bar{U}_a = (-1, \sqrt{\alpha}, \sqrt{\beta}, 0)$ ) and neglecting terms like  $h_{00(1)}\bar{U}^a$  (because they are second order terms), the expression becomes

$$\begin{aligned}
\bar{E}_\gamma \propto & \frac{1}{2} \int \bar{g}_{bc,0} \bar{U}^b \bar{U}^c dw - \frac{1}{4} h_{00} \int \bar{g}_{bc,0(0)} \bar{U}^b {}_{(0)}\bar{U}^c dw + {}_{(0)}\bar{U}_0 \\
& - \frac{1}{2} {}_{(0)}\bar{U}_0 h_{00} + \vec{U} \cdot \vec{V} + \frac{1}{2} \int \bar{g}_{bc,i(0)} \bar{U}^b {}_{(0)}\bar{U}^c dw \bar{V}^i. \quad (11)
\end{aligned}$$

The last term of the right hand side vanishes, because for  $i = r$  and  $i = \phi \Rightarrow \bar{g}_{bc,i} = 0$  and also because  $\bar{U}^\phi = 0$ . The term

$$\begin{aligned}
& \frac{1}{4} h_{00} \int \bar{g}_{bc,0(0)} \bar{U}^b {}_{(0)}\bar{U}^c dw = \frac{1}{4} h_{00} \int \bar{g}_{bc,0(0)} \bar{U}^b {}_{(0)}\bar{U}^c dw \\
& = \frac{1}{4} h_{00} \int \bar{g}_{\theta\theta,\eta} ({}_{(0)}\bar{U}^\theta)^2 dw = \frac{1}{2} h_{00} \int \frac{b^2}{a^2} \left( \frac{\dot{b}}{b} - \frac{\dot{a}}{a} \right) ({}_{(0)}\bar{U}^\theta)^2 dw,
\end{aligned}$$

may be numerically computed. Here the dot represents a derivative with respect to conformal time:  $(\dot{\phantom{x}}) \equiv \frac{d}{d\eta}$ . If we choose accurately the values of density parameters  $\Omega_M$  and  $\Omega_\Lambda$  (see Aguiar & Crawford [6]) such that  $\Omega_M + \Omega_\Lambda \simeq 1$  this integral may be neglected, because it is a first order term times another first order quantity (see [7]). The first term in the right hand side may be decomposed by the following way

$$\begin{aligned} & \frac{1}{2} \int \bar{g}_{bc,0} \bar{U}^b \bar{U}^c dw \\ &= \frac{1}{2} \int \bar{g}_{bc,0(0)} \bar{U}^b_{(0)} \bar{U}^c dw + \frac{1}{2} \int \bar{g}_{bc,0(0)} \bar{U}^b_{(1)} \bar{U}^c dw + \frac{1}{2} \int \bar{g}_{bc,0(1)} \bar{U}^b_{(0)} \bar{U}^c dw \\ &= \frac{1}{2} \int \bar{g}_{bc,0(0)} \bar{U}^b_{(0)} \bar{U}^c dw + \int \bar{g}_{\theta\theta,\eta(0)} \bar{U}^\theta_{(1)} \bar{U}^\theta dw. \end{aligned}$$

But

$$\int \bar{g}_{\theta\theta,\eta(0)} \bar{U}^\theta_{(1)} \bar{U}^\theta dw = 2 \int \frac{b^2}{a^2} \left( \frac{\dot{b}}{b} - \frac{\dot{a}}{a} \right)_{(0)} \bar{U}^\theta_{(1)} \bar{U}^\theta dw,$$

may also be neglected for the reason pointed previously. Thus,

$$\bar{E}_\gamma \propto \frac{1}{2} \int \bar{g}_{bc,0(0)} \bar{U}^b_{(0)} \bar{U}^c dw + {}_{(0)}\bar{U}_0 - \frac{1}{2} {}_{(0)}\bar{U}_0 h_{00} + \vec{\bar{U}} \cdot \vec{\bar{V}}. \quad (12)$$

Calculating the ratio of energies in the emission instant ( $e$ ) and in the reception instant ( $r$ ) we obtain

$$\frac{\bar{E}_{\gamma_e}}{\bar{E}_{\gamma_r}} = \frac{(\bar{U}_a \bar{V}^a)|_e}{(\bar{U}_a \bar{V}^a)|_r} = \frac{-1 + \frac{1}{2} h_{00}|_e + (\vec{\bar{U}} \cdot \vec{\bar{V}})|_e}{-1 + \frac{1}{2} h_{00}|_r + (\vec{\bar{U}} \cdot \vec{\bar{V}})|_r + \frac{1}{2} \int_e^r \bar{g}_{bc,0(0)} \bar{U}^b_{(0)} \bar{U}^c dw}, \quad (13)$$

(the symbol  $X|_A$  means that  $X$  is being evaluated at point  $A$ ). Considering the approximation  $(1 + X)^{-1} \simeq 1 - X$  we have

$$\frac{\bar{E}_{\gamma_e}}{\bar{E}_{\gamma_r}} = 1 + \frac{1}{2} [h_{00}]_e^r + [\vec{\bar{U}} \cdot \vec{\bar{V}}]_e^r + \frac{1}{2} \int_e^r \bar{g}_{bc,0(0)} \bar{U}^b_{(0)} \bar{U}^c dw, \quad (14)$$

where  $[X]_A^B \equiv X(B) - X(A)$ . The result obtained in  $d\bar{s}^2$  may be transported to  $ds^2$  using the relation  $E(t) = \frac{1}{a(t)} \bar{E}(w)$ , as can easily be obtained. The photon redshift between emission at the point  $e$  in the LSS and reception at the point  $r$  is given by the ratio of the measured energies at emission and reception,

$$z + 1 = \frac{\lambda_r}{\lambda_e} = \frac{E(t_e)}{E(t_r)} = \frac{a_r}{a_e} \frac{\bar{E}(w_e)}{\bar{E}(w_r)}. \quad (15)$$

On the other hand, the redshift is also given by the ratio of the black body associated temperatures at the emission and reception times,

$$\frac{T_e}{T_r} = z + 1. \quad (16)$$

Taking these last two equations, and considering again a linear approximation one obtains

$$\begin{aligned} T_r &\simeq \frac{a_e}{a_r} T_e \left[ 1 - \frac{1}{2} [h_{00}]_e^r - [\vec{U} \cdot \vec{V}]_e^r - \frac{1}{2} \int_e^r \bar{g}_{bc,0(0)} \bar{U}^b_{(0)} \bar{U}^c dw \right] \\ &= \frac{a_e}{a_r} T_e \left( 1 + \frac{\delta T_{\text{journey}}}{T_{\text{journey}}} \right), \end{aligned} \quad (17)$$

so to evaluate the observed anisotropy we must take into account the journey and emission perturbations (see [17] p.357), and write it as

$$\frac{\delta T_r}{T_r} = \frac{\delta T_e}{T_e} + \frac{\delta T_{\text{journey}}}{T_{\text{journey}}} \quad (18)$$

or equivalently,

$$\frac{\delta T_r}{T_r} = \frac{\delta T_e}{T_e} - \frac{1}{2} [h_{00}]_e^r - [\vec{U} \cdot \vec{V}]_e^r - \frac{1}{2} \int_e^r \bar{g}_{bc,0(0)} \bar{U}^b_{(0)} \bar{U}^c dw. \quad (19)$$

Now let us define the perturbations  $h_{ab}$ . These fluctuations are *gauge* dependent. This means that one must make a gauge choice which involves fixing the constant-time hypersurfaces (and the spatial grid on these surfaces) where these fluctuations are defined [18, 19]. As it is widely assumed, we will choose a conformal *Newtonian gauge* to allow a more intuitive understanding. Considering only scalar perturbations, the non zero quantities are (see [18] Equations (2.9) and (3.21),  $B = E = 0$  for the longitudinal gauge)

$$h_{00} = 2\Psi; \quad h_{11} = h_{22} = h_{33} = 2\Phi. \quad (20)$$

As it was previously stated, these scalar quantities are functions of time and position,  $\Psi = \Psi(\eta, x^i)$ ,  $\Phi = \Phi(\eta, x^i)$  and they may be seen as a Newtonian potential and a spatial curvature perturbation potential, respectively [18, 19].

For our models, we have perfect fluid, so the anisotropic pressure is null. This implies that  $\Psi = -\Phi$  (see [19] for details). Writing (19) in the Newtonian gauge we obtain,

$$\begin{aligned} \frac{\delta T_r}{T_r} &= \frac{\delta T_e}{T_e} - [\Psi]_e^r - [\vec{U} \cdot \vec{V}]_e^r - \frac{1}{2} \int_e^r \left\{ [-h_{00,0(0)} \bar{U}^\eta]^2 + h_{11,0(0)} \bar{U}^r]^2 \right. \\ &\quad \left. + \frac{b^2}{a^2} h_{22,0(0)} \bar{U}^\theta]^2 \right\} dw - \int_e^r (1 + h_{22}) \frac{b^2}{a^2} \left( \frac{\dot{b}}{b} - \frac{\dot{a}}{a} \right)_{(0)} \bar{U}^\theta]^2 dw \end{aligned} \quad (21)$$

The last term of the right hand side may be neglected, as it is shown in [7]. So, we get

$$\begin{aligned} \frac{\delta T_r}{T_r} &= \frac{\delta T_e}{T_e} - [\Psi]_e^r - [\vec{U} \cdot \vec{V}]_e^r \\ &\quad - \int_e^r \left\{ -\frac{\partial \Psi}{\partial \eta}_{(0)} \bar{U}^\eta]^2 + \frac{\partial \Phi}{\partial \eta} \left[ (\bar{U}^r)^2 + \frac{b^2}{a^2} (\bar{U}^\theta)^2 \right] \right\} dw, \end{aligned} \quad (22)$$

or,

$$\frac{\delta T_r}{T_r} = \frac{\delta T_e}{T_e} - [\Psi]_e^r - \left[ \vec{U} \cdot \vec{V} \right]_e^r + 2 \int_e^r \frac{\partial \Psi}{\partial \eta} dw, \quad (23)$$

as can easily be shown. Now, we should spell out the physical interpretation of each one of the three factors of the right hand side of previous equation. When matter and radiation are decoupled, free CMBR photons, climbing the gravitational potential generated by density perturbations, undergo a gravitational redshift, with corresponding loss of energy. The photon energy variation in this process is given by the term  $[\Psi]_e^r \equiv \Psi(r) - \Psi(e)$ . The second term,  $\left[ \vec{U} \cdot \vec{V} \right]_e^r \equiv \vec{U} \cdot (\vec{V}(r) - \vec{V}(e))$ , corresponds to the Doppler effect induced by the relative motion of the observer in the emission and reception events. The Doppler term has an observational meaning of a dipolar anisotropy ( $\vec{U} \cdot \vec{V}(r)$ ) on CMBR temperature and is usually removed from the equation and dealt with separately. The other term ( $\vec{U} \cdot \vec{V}(e)$ ) can be dropped for large angular scales (for details see [17] p.124 and p.84). The last term tells us that the perturbing potential may vary between the emission and reception instants.

For flat FLRW models without cosmological constant,  $\Psi$  is time constant [16, 18], so the last term in the right hand side of Equation (23) vanishes. In our case the cosmological constant is not vanishing, and indeed  $\Lambda$  plays an important role in our analysis. Taking into account recent observations [20, 21] which suggest  $\Omega_0 \sim 0.3$  and  $\Omega_{\Lambda_0} \sim 0.7$ , we consider values such that  $\Omega_0 + \Omega_{\Lambda_0} \simeq 1$  (see [7]).

Now, we may explicitly compute the intrinsic temperature fluctuations  $\delta T_e/T_e$ , originated by the set of physical and microphysical processes, associated to density perturbations in LSS. Despite its youth, the Universe is already highly isotropic (shear  $\Sigma \ll 1$ ). Then, for simplicity, we assume in this section that the Universe might be characterized by a flat FLRW model. Because the density fluctuations are very small, we may treat them in the context of linear theory of perturbations using Stefan-Boltzmann law

$$\rho_\gamma = \sigma_{SB} T^4, \quad (24)$$

where  $\sigma_{SB}$  is a constant and  $\rho_\gamma$  is the radiation density. Differentiating this equation one easily obtains

$$\frac{\delta T_e}{T_e} = \frac{1}{4} \frac{\delta \rho_\gamma}{\rho_\gamma}. \quad (25)$$

At this time, when the Universe is very young, the total energy density is not only due to radiation. The baryonic matter plays an identical role, and so the matter density  $\rho_m$  is related with  $\rho_\gamma$  by

$$\frac{\delta \rho_m}{\rho_m} - \frac{3}{4} \frac{\delta \rho_\gamma}{\rho_\gamma} = 0, \quad (26)$$



if the perturbation mode is adiabatic and on scales larger than the horizon at this time [22]. Then, for perturbations on scales greater than the horizon we may write

$$\frac{\delta T_e}{T_e} = \frac{1}{3} \frac{\delta \rho_m}{\rho_m}. \quad (27)$$

From the last expression we see that, for adiabatic perturbations, the over-density (under-density) regions are intrinsically hotter (colder) than the LSS mean temperature. According with [16, 18],  $\delta \rho_m / \rho_m = -2\Psi + \mathcal{O}[(k/H)^2]$ , where  $k$  is the momentum associated to perturbation scale and  $H$  the Hubble parameter<sup>2</sup>. The larger is the scale, the smaller is  $k$ , so, for perturbations greater than the horizon  $k \ll H$ , the over-density locals coincide with the potential well, because,

$$\frac{\delta T_e}{T_e} \simeq -\frac{2}{3} \Psi_e. \quad (28)$$

We may rewrite equation (23), where without loss of generality we put  $\Psi_r = 0$ . This equation is valid if the observation is made for regions with angular scales containing the horizon ( $\vartheta \gtrsim 2^\circ$ ) in recombination epoch. Finally we recover the Sachs-Wolfe result

$$\frac{\delta T_r}{T_r} = \frac{1}{3} \Psi_e + 2 \int_e^r \frac{\partial \Psi}{\partial \eta} dw. \quad (29)$$

The second term is called the *integrated Sachs-Wolfe effect*. As it was expected, this expression for the Sachs-Wolfe effect is the same as the one obtained for FLRW universes, for the same order of approximation, and for adiabatic initial conditions.

### 3 Study of the behavior of the $\mathcal{W}$ , $\dot{\mathcal{W}}$ , $\Sigma$ and $\dot{\Sigma}$

As mentioned earlier in this article, we have two scalar,  $\mathcal{W}$  and  $\Sigma$  or its square, we can say how 'close' to FLRW are our models. When not only one, but two parameters are close to zero, can say that our models are 'close' to FLRW [2]. Thus, we study the behavior of both, and as their time derivatives. As for our models, with perfect fluid, the magnetic part of Weyl is null we obtain for  $\mathcal{W}$  from (1), after some simplification

$$\mathcal{W} = \frac{1}{3H^2} \left( \frac{\ddot{a}}{a} - \frac{\ddot{b}}{b} \right), \quad (30)$$

or also

$$\mathcal{W} = \frac{1}{6} \frac{H_{b_0}^2}{H^2} \left[ \frac{\Omega_{M_0}}{2} \left( \frac{3}{y^3} - \frac{1}{xy^2} \right) + \Omega_{\Lambda_0} \frac{1}{xy^2} - \frac{H_{a_0}}{H_{b_0}} \frac{1}{xy^2} \right], \quad (31)$$

where  $H$  is, in our case, the average value of two Hubble parameter,  $H = (\dot{a}/a + 2\dot{b}/b)/3$ . Thus, we can deriving both terms in the equation above, obtaining

---

<sup>2</sup>Nevertheless our models have two Hubble parameters  $H_a$  and  $H_b$ , they have practically the same value  $H_a \simeq H_b \simeq H$  due to our parameters choose.

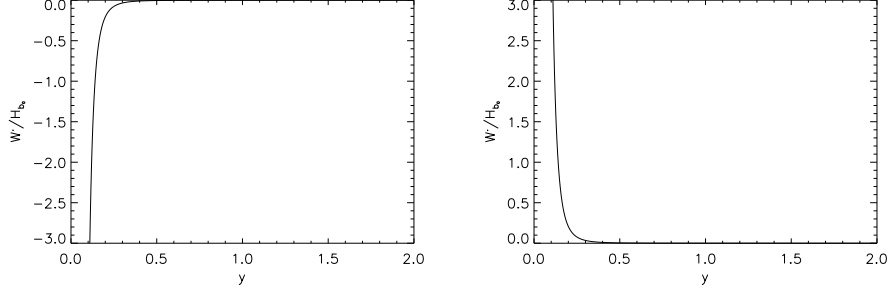


Figure 1: On the left: Variation of  $\dot{W}$  relative to scale factor  $y = b(t)/b_0$  in Kantowski-Sachs model, with the values  $\Omega_{M_0} = 0.3$  and  $\Omega_{\Lambda_0} = 0.7 + 1 \times 10^{-3}$ . It is clear the asymptotic behavior of the  $\dot{W}$  ( $\dot{W} \rightarrow -\infty$ ), when  $y \rightarrow 0$ , that is, when we go back in time. Unlike  $\dot{W} \rightarrow 0$  for  $y > 1$  values. Note that  $y = 1$  corresponds to the current instant of the Universe.

Figure 2: On the right: Variation of  $\dot{W}$  relative to scale factor  $y = b(t)/b_0$  in Bianchi type-III model, with the values  $\Omega_{M_0} = 0.3$  and  $\Omega_{\Lambda_0} = 0.7 - 1 \times 10^{-3}$ . We see from the figure that  $\dot{W} \rightarrow +\infty$  when  $t \rightarrow 0$ . For  $y > 1$  values  $\dot{W}$  converges quickly to zero. Apart from an opposite sign,  $\dot{W}$  has a very similar behavior in both models.

$$\begin{aligned} \frac{\dot{W}}{H_{b_0}} = & -\frac{\left(\frac{\ddot{x}}{x} + 2\frac{\ddot{y}}{y} - \frac{\dot{x}^2}{x^2} - 2\frac{\dot{y}^2}{y^2}\right)}{\left(\frac{\dot{x}}{x} + 2\frac{\dot{y}}{y}\right)} \mathcal{W} + \left[ \frac{\Omega_{M_0}}{2} \left( -\frac{9}{y^3} \frac{\dot{y}}{y} + \frac{1}{xy^2} \frac{\dot{x}}{x} + \frac{2}{xy^2} \frac{\dot{y}}{y} \right) + \right. \\ & \left. \Omega_{\Lambda_0} \left( -\frac{1}{xy^2} \frac{\dot{x}}{x} - \frac{2}{xy^2} \frac{\dot{y}}{y} \right) + \frac{H_{a_0}}{H_{b_0}} \left( \frac{1}{xy^2} \frac{\dot{x}}{x} \frac{2}{xy^2} \frac{\dot{y}}{y} \right) \right], \end{aligned} \quad (32)$$

Using the equations

$$\dot{y} = \pm H_{b_0} \sqrt{\Omega_{M_0} \left( \frac{1}{y} - 1 \right) + \Omega_{\Lambda_0} (y^2 - 1) + 1}, \quad (33)$$

and

$$\dot{x} = H_{b_0} \frac{\frac{\Omega_{M_0}}{2} \left( 1 - \frac{x}{y} \right) + \Omega_{\Lambda_0} (-1 + xy^2) + \frac{H_{a_0}}{H_{b_0}}}{y \sqrt{\Omega_{M_0} \left( \frac{1}{y} - 1 \right) + \Omega_{\Lambda_0} (y^2 - 1) + 1}}, \quad (34)$$

respectively (2.12) and (2.22) obtained in Aguiar & Crawford [6] we integrate numerically in time the equations  $\dot{W}$  and  $\mathcal{W}$  and we draw some graphs. For the Kantowsky-Sachs model we chose the values  $\Omega_{M_0} = 0.3$  and  $\Omega_{\Lambda_0} = 0.7 + 1 \times 10^{-3}$  and in Bianchi type-III model we chose  $\Omega_{M_0} = 0.3$  and  $\Omega_{\Lambda_0} = 0.7 - 1 \times 10^{-3}$ . It is clearly seen in the figures that if we walk backwards in time we see that  $\dot{W}$  diverges to  $-\infty$  in the Kantowsky-Sachs model and  $+\infty$  in Bianchi type-III model. This behavior reinforces the fact that  $\mathcal{W}$  diverge when we go back in time. In the Kantowski-Sachs model  $\mathcal{W} \rightarrow +\infty$  when  $t \rightarrow 0$  and in Bianchi type-III model  $\mathcal{W} \rightarrow -\infty$  when  $t \rightarrow 0$ . From equation (31), and again using the equations (2.12) and (2.22)

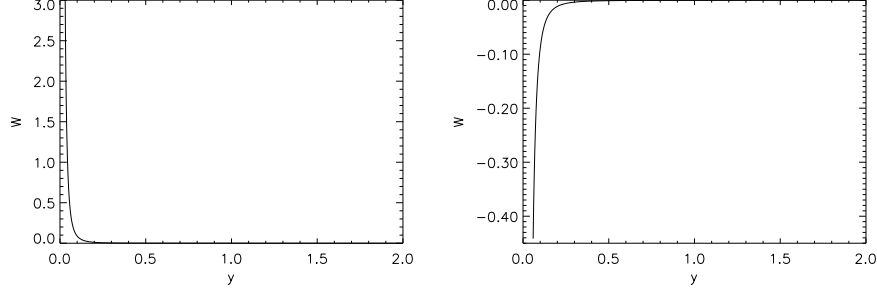


Figure 3: On the left: Variation of  $\mathcal{W}$  against the scale factor  $y = b(t)/b_0$  in Kantowski-Sachs model, with the values  $\Omega_{M_0} = 0.3$  and  $\Omega_{\Lambda_0} = 0.7 + 1 \times 10^{-3}$ . It is seen in this figure that  $\mathcal{W}$  remains very close to zero for a certain period, but from a given value of  $y$  close to zero, this grows asymptotically. The  $y$  value from which their growth is asymptotic will be more close to zero as closer to the unit is the sum of the two density parameters. For  $y > 1$  values  $\mathcal{W}$  vanishes rapidly.

Figure 4: On the right: Variation of  $\mathcal{W}$  against the scale factor  $y = b(t)/b_0$  in Bianchi type-III model, with the values  $\Omega_{M_0} = 0.3$  and  $\Omega_{\Lambda_0} = 0.7 - 1 \times 10^{-3}$ . We see in the figure that  $\mathcal{W}$  remains very close to zero for a certain period, but from a given value and  $y$  close to zero,  $y$  diverges asymptotically. The  $y$  value from which their growth is asymptotic will be more close to zero as closer to the unit is the sum of the two density parameters. The  $\mathcal{W}$  value in modulus has a very similar behavior in both models. For  $y > 1$  values,  $\mathcal{W}$  rapidly vanishes.

in Aguiar & Crawford [6], we see that  $\mathcal{W}$  goes to zero when  $x$  and  $y$  goes to infinity. If we want to relate  $\dot{\mathcal{W}}$  with  $\mathcal{W}$ , we see once again that in both these models the two scalars diverge when we walk back in time, although  $\dot{\mathcal{W}}$  diverges more sharply than  $\mathcal{W}$ .

Let us study then the behavior of  $\Sigma$ . From the equation (2) the expression of  $\Sigma$  for our models, with perfect fluid is

$$\Sigma = \frac{1}{3} \frac{1}{H} \left( \frac{\dot{a}}{a} - \frac{\dot{b}}{b} \right). \quad (35)$$

Deriving both members we obtain easily

$$\dot{\Sigma} = - \frac{\left( \frac{\ddot{x}}{x} + 2 \frac{\ddot{y}}{y} - \frac{\dot{x}^2}{x^2} - 2 \frac{\dot{y}^2}{y^2} \right)}{\left( \frac{\dot{x}}{x} + 2 \frac{\dot{y}}{y} \right)} \Sigma + \frac{\frac{\ddot{x}}{x} - \frac{\ddot{y}}{y} - \frac{\dot{x}^2}{x^2} + \frac{\dot{y}^2}{y^2}}{\left( \frac{\dot{x}}{x} + 2 \frac{\dot{y}}{y} \right)}. \quad (36)$$

Using back to equations (2.12), (2.22) from Aguiar & Crawford [6] we have integrated numerically in order to time the equations  $\dot{\Sigma}$  and  $\Sigma$  and got some graphs illustrative of these behavior. Also the scalar  $\Sigma$  has a behavior highly divergent when we stepped back in time and highly convergent to zero when we consider values of scale factors  $y \sim 1$  in both models. This behavior is strongly supported by the behavior of its derivative  $\dot{\Sigma}$ .

Both in the study of the scalar  $\mathcal{W}$  as the study of  $\Sigma$ , we use density parameter values  $|\Omega_{M_0} + \Omega_{\Lambda_0} - 1| = 1 \times 10^{-3}$ , just to illustrate the qualitative

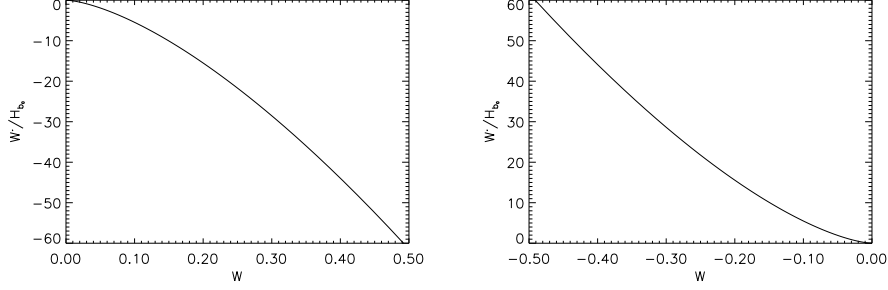


Figure 5: On the left: Variation of  $\dot{\mathcal{W}}$  depending on  $\mathcal{W}$  to Kantowski-Sachs model, with values  $\Omega_{M_0} = 0.3$  and  $\Omega_{\Lambda_0} = 0.7 + 1 \times 10^{-3}$ . As we go back in time both scalar diverge, and  $\dot{\mathcal{W}}$  a more pronounced divergence. When  $t \rightarrow \infty$ ,  $\dot{\mathcal{W}}$  and  $\mathcal{W}$  vanishes.

Figure 6: On the right: Variation of  $\dot{\mathcal{W}}$  depending on  $\mathcal{W}$  to Bianchi type-III model, with values  $\Omega_{M_0} = 0.3$  and  $\Omega_{\Lambda_0} = 0.7 - 1 \times 10^{-3}$ . As we go back in time both scalar values diverge although by symmetrical values to the Kantowski-Sachs model. When  $t \rightarrow \infty$ ,  $\dot{\mathcal{W}}$  and  $\mathcal{W}$  vanishes.

behavior of both models. However, if we choose values for density parameters of the order of  $|\Omega_{M_0} + \Omega_{\Lambda_0} - 1| \simeq 10^{-9}$  and making  $H_{a_0}/H_{b_0} \pm 3.6 \times 10^{-9}$  we obtain the following values:

$$\mathcal{W}_0 \sim 2 \times 10^{-10} \quad \text{e} \quad \mathcal{W}_{ls} \sim 3.8 \times 10^{-1} \quad (37)$$

and

$$\Sigma_0 \sim -3.6 \times 10^{-9} \quad \text{e} \quad \Sigma_{ls} \sim -4.4 \times 10^{-5} \quad (38)$$

in Kantowski-Sachs model and

$$\mathcal{W}_0 \sim -2 \times 10^{-10} \quad \text{e} \quad \mathcal{W}_{ls} \sim -5.6 \times 10^{-1}. \quad (39)$$

and

$$\Sigma_0 \sim 3.6 \times 10^{-9} \quad \text{e} \quad \Sigma_{ls} \sim 6.5 \times 10^{-5} \quad (40)$$

in Bianchi type-III model.

The behavior of these scalar clearly shows that we can keep close to our models from FLRW behavior provided that the appropriate density parameter settings and Hubble parameters are close to the present time. However, going back to “last scattering” time these models exhibit strongly anisotropic behavior.

## 4 Concluding Remarks

We stress once more we should bear in mind that the assumption  $H_a \simeq H_b$  does not imply, by itself, an isotropic or even an almost isotropic metric, as it is expressed by the growth of Weyl term in Equations (1) and (2), when we go back in time to the last scattering epoch. Although the  $\Sigma$  term remains at a low value from the present ( $\Sigma_0 \sim -3.6 \times 10^{-9}$ ) to the last scattering

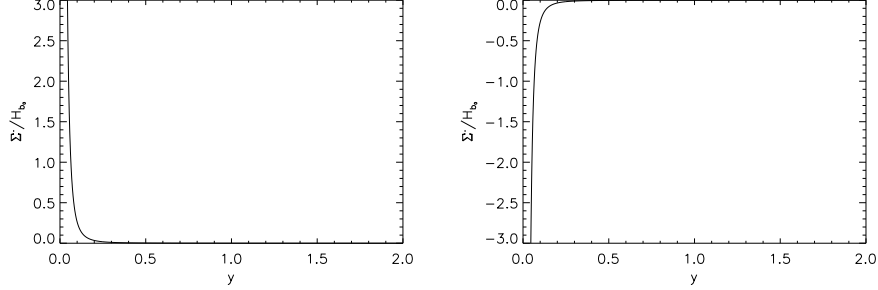


Figure 7: On the left: Variation of  $\dot{\Sigma}$  against the scale factor  $y = b(t)/b_0$  in Kantowski-Sachs model, with values  $\Omega_{M_0} = 0.3$  and  $\Omega_{\Lambda_0} = 0.7 + 1 \times 10^{-3}$ . It is clear the asymptotic behavior of  $\dot{\Sigma}$  ( $\dot{\Sigma} \rightarrow -\infty$ ), when  $y \rightarrow 0$ , ie when we go back in time. Unlike  $\dot{\mathcal{W}} \rightarrow 0$  for  $y > 1$  values. Note that  $y = 1$  corresponds to the present time in Universe.

Figure 8: On the right: Variation of  $\dot{\Sigma}$  against the scale factor  $y = b(t)/b_0$  in Bianchi type-III model, the values  $\Omega_{M_0} = 0.3$  and  $\Omega_{\Lambda_0} = 0.7 - 1 \times 10^{-3}$ . We see from the figure that  $\dot{\Sigma} \rightarrow +\infty$  when  $t \rightarrow 0$ . For  $y > 1$  values  $\dot{\Sigma}$  converges quickly to zero. We see that  $|\dot{\Sigma}|$  has a behavior very similar in both models.

epoch ( $\Sigma_{ls} \sim -4.4 \times 10^{-5}$ ), the Weyl term, grows from  $\mathcal{W}_0 \sim 2 \times 10^{-10}$  at the present to  $\mathcal{W}_{ls} \sim 3.8 \times 10^{-1}$  at the last scattering time. This shows the anisotropic character of these models in the past. Summarizing,  $\Sigma$  grows about  $1.2 \times 10^4$ , while  $\mathcal{W}$  grows about  $1.9 \times 10^9$ , when we go back in time ( $t_0 \rightarrow t_{ls}$ ). Even though we impose a high level of isotropy at present time, the anisotropic behavior of these models comes forward as we go back in time. Nevertheless, the growth of  $\mathcal{W}$  term does not affect decisively the first order computation of  $\delta T_r/T_r$  term.

These results could lead us to conclude that the accuracy in density parameter settings and Hubble parameters ( $H_a$  e  $H_b$ ) introduced was so high that these models were ‘transformed’ in isotropic models and therefore of no interest study. The behavior of the scalar  $\mathcal{W}$  and  $\Sigma$  and their time derivatives has allowed to conclude that in fact these models can display a high level isotropy for a period of time too high since that  $\mathcal{W}$  and  $\Sigma$  can remain approximately zero. But if we go back in time to very early times, these scalar tends to infinity, regardless of the precision to choose the parameters of Hubble and density, which shows the anisotropic nature of these models.

Since the obtained expression (for Sachs-Wolfe effect) is the same as the one given for FLRW flat model, we may conclude that, these anisotropic models are also good candidates to the description of observed Universe provided we may assume  $H_{a_0} \simeq H_{b_0}$  (taking into account the upper bound on the present value of the shear parameter imposed by COBE observations) and a particular choice of the density parameters:  $\Omega_0 + \Omega_{\Lambda_0} \simeq 1$ , (see [7]). This is another step taken in the same direction as in [6]. This is also in agreement with another previous result: it is not possible to distinguish a Kantowski-Sachs model from the FLRW models, with the classical tests of

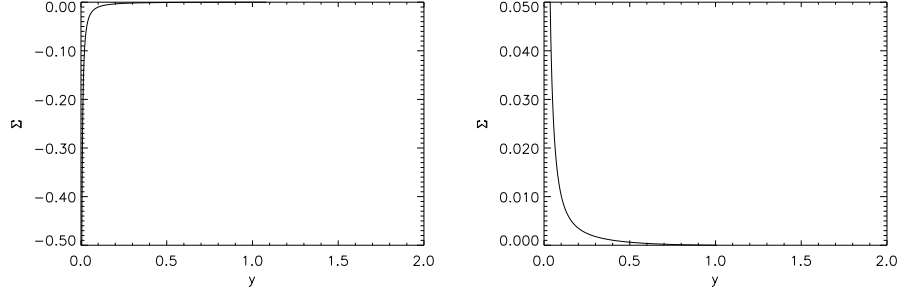


Figure 9: On the left: Variation of  $\Sigma$  against the scale factor  $y = b(t)/b_0$  in Kantowski-Sachs model, with values  $\Omega_{M_0} = 0.3$  and  $\Omega_{\Lambda_0} = 0.7 + 1 \times 10^{-3}$ . It is seen in this figure  $\Sigma$  remains very close to zero for a certain period, but from a given value of  $y$  close to zero, this increases asymptotically. The value  $y$  from which their growth is asymptotic will be more close to zero as closer to the unit is the sum of the two density parameters. For  $y > 1$  values  $\Sigma$  vanishes quickly.

Figure 10: On the right: Variation of  $\Sigma$  against the scale factor  $y = b(t)/b_0$  in Bianchi type-III model, the values  $\Omega_{M_0} = 0.3$  and  $\Omega_{\Lambda_0} = 0.7 - 1 \times 10^{-3}$ . It is seen in this figure  $\Sigma$  remains very close to zero for a certain period, but from a given value of  $y$  close to zero, this diverges asymptotically. The  $y$  value from which their growth is asymptotic will be more close to zero as closer to the unit is the sum of the two density parameters. The  $|\Sigma|$  has a behavior very similar in both models. For  $y > 1$  values  $\Sigma$  quickly vanishes.

Cosmology, if the Hubble parameters along the orthogonal directions are assumed to be approximately equal [5].

In future work we intend to use Planck satellite data [23] and interferometer AMIBA [24], which will provide much better resolution and which will require to consider the integrated Sachs-Wolfe effect.

In conclusion, the observation of Sachs-Wolfe effect plateau does not permit us to distinguish between FLRW models and the anisotropic Kantowski-Sachs and Bianchi type-III models. To investigate this in more detail, it is necessary to consider and process the data from Planck [23] and AMIBA [24] projects to regions smaller than the horizon at the last scattering ( $\ell > 100$ ,  $\vartheta < 1^\circ$ ). Within this region of multipoles, perturbations are model dependent. Only with this information we may conclude finally whether our Universe can be modeled by one of these anisotropic models. This will be the purpose of further work.

## Acknowledgements

The authors thank A. Barbosa Henriques, Ant3nio da Silva and Andrew Liddle for useful discussions and comments. This work was supported in part by grants BD 971 and BD/11454/97 PRAXIS XXI, from JNICT, CERN/P/FIS/40131/2000 Project and by PEst-OE/FIS/UI2751/2011 Project from FCT.

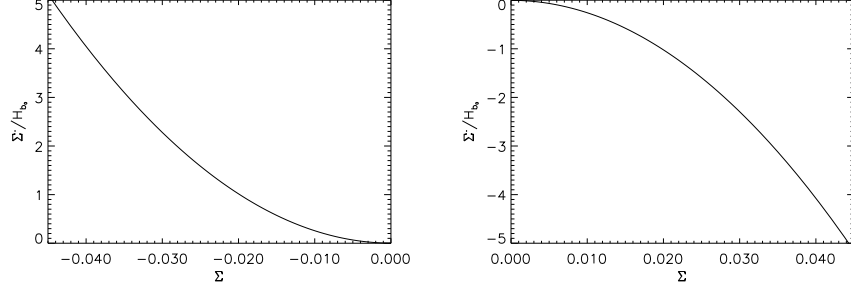


Figure 11: On the left: Variation of  $\dot{\Sigma}$  as a function of  $\Sigma$ , to Kantowski-Sachs model, with values  $\Omega_{M_0} = 0.3$  and  $\Omega_{\Lambda_0} = 0.7 + 1 \times 10^{-3}$ . When we go back in time both scalar diverge, and  $\dot{\Sigma}$  as a more pronounced divergence. When  $t \rightarrow \infty$ ,  $\dot{\Sigma}$  and  $\Sigma$  tend to zero.

Figure 12: On the right: Variation of  $\dot{\Sigma}$  as a function of  $\Sigma$ , to Bianchi type-III model, with values  $\Omega_{M_0} = 0.3$  and  $\Omega_{\Lambda_0} = 0.7 - 1 \times 10^{-3}$ . When we go back in time both scalar diverge although by symmetrical values of Kantowski-Sachs model. When  $t \rightarrow \infty$ ,  $\dot{\Sigma}$  and  $\Sigma$  tend to zero.

## References

- [1] J. Ehlers, P. Geren and R. K. Sachs, *J. Math. Phys.* **9**, 1344 (1968).
- [2] U. S. Nilsson *et. al.*, *Astrophys. J.* **522** L1 (1999).
- [3] W. R. Stoeger, R. Maartens and G. F. R. Ellis, *Astrophys. J.* **443** 1 (1995).
- [4] W. C. Lim *et. al.*, *Class. Quantum Grav.* **18**, 5583 (2001).
- [5] A. Henriques, *Astrophysics and Space Science* **235** 129 (1996).
- [6] P. Aguiar and P. Crawford, *Phys. Rev. D* **62** 123511 (2000).
- [7] P. Aguiar and P. Crawford, “Numerical Cumputation of an Integral”  
<http://cosmo.fis.fc.ul.pt/~paguiar/intcomput.pdf>
- [8] A. A. Penzias and R. W. Wilson, *Astrophys. J.* **142** 419 (1965).
- [9] G. F. Smoot, *Astrophys. J.* **396** L1 (1992).
- [10] P. Coles and F. Lucchin, *Cosmology – The Origin and Evolution of Cosmic Structure* (Wiley, Chichester, England 1995), p. 185.
- [11] J. C. Mather *et. al.*, *Astrophys. J.* **420** 439 (1994).
- [12] R. B. Partridge, *Class. Quant. Grav.* **11** A153 (1994).
- [13] R. B. Partridge, *Rep. Prog. Phys.* **51** 647 (1988).
- [14] R. K. Sachs and A. M. Wolfe, *Astrophys. J.* **147** 73 (1967).

- [15] C. B. Collins and S. W. Hawking, *Mon. Not. Astron. Soc.* **162** 307 (1973).
- [16] M. White *et. al.*, *Ann. Rev. Astron. & Astrophys.* **32** 319 (1994).
- [17] A. R. Liddle and D. H. Lyth, *Cosmological Inflation and Large-Scale Structure* (Cambridge University Press, Cambridge, 2000).
- [18] V. F. Mukhanov *et. al.*, *Phys. Reports* **215** 203 (1992).
- [19] W. Hu, Ph.D Thesis, Univ. of California, Berkeley, 1995, Chapter 4.
- [20] S. Perlmutter *et. al.*, *Nature* **391** 51 (1998).
- [21] A. G. Riess *et. al.*, *Astron. J.* **116** 1009 (1998).
- [22] E. W. Kolb and M. S. Turner, *The Early Universe* (Addison-Wesley Publishing Company, 1990), Chapter 9.2.
- [23] <http://www.esa.int/SPECIALS/Planck/index.html>
- [24] <http://amiba.asiaa.sinica.edu.tw/>
- [25] E. Martinez-Gonzalez and J.L. Sanz, *Astron. & Astrophys.* **300** (1995) 346.
- [26] R. Maartens *et. al.*, *Astron. & Astrophys.* **309** (1996) L7.